

# SANDIA REPORT

SAND97-1333 • UC-704

Unlimited Release

Printed May 1997

## Target Fabrication for Ion-Beam Driven Hohlraum Experiments

J. H. Aubert, P. S. Sawyer, M. L. Smith

Prepared by  
Sandia National Laboratories  
Albuquerque, New Mexico 87185 and Livermore, California 94550

Sandia is a multiprogram laboratory operated by Sandia  
Corporation, a Lockheed Martin Company, for the United States  
Department of Energy under Contract DE-AC04-94AL85000.

Approved for public release; distribution is unlimited.



Issued by Sandia National Laboratories, operated for the United States Department of Energy by Sandia Corporation.

**NOTICE:** This report was prepared as an account of work sponsored by an agency of the United States Government. Neither the United States Government nor any agency thereof, nor any of their employees, nor any of their contractors, subcontractors, or their employees, makes any warranty, express or implied, or assumes any legal liability or responsibility for the accuracy, completeness, or usefulness of any information, apparatus, product, or process disclosed, or represents that its use would not infringe privately owned rights. Reference herein to any specific commercial product, process, or service by trade name, trademark, manufacturer, or otherwise, does not necessarily constitute or imply its endorsement, recommendation, or favoring by the United States Government, any agency thereof or any of their contractors or subcontractors. The views and opinions expressed herein do not necessarily state or reflect those of the United States Government, any agency thereof or any of their contractors.

Printed in the United States of America. This report has been reproduced directly from the best available copy.

Available to DOE and DOE contractors from  
Office of Scientific and Technical Information  
PO Box 62  
Oak Ridge, TN 37831

Prices available from (615) 576-8401, FTS 626-8401

Available to the public from  
National Technical Information Service  
US Department of Commerce  
5285 Port Royal Rd  
Springfield, VA 22161

NTIS price codes  
Printed copy: A08  
Microfiche copy: A01

SAND97-1333  
Unlimited Release  
Printed May 1997

Distribution  
Category UC- 704

Target Fabrication for Ion-Beam  
Driven Hohlraum Experiments

J. H. Aubert, P. S. Sawyer  
Encapsulants and Porous Materials Department  
Sandia National Laboratories  
P.O. Box 5800  
Albuquerque, NM 87185-1407

and

M. L. Smith  
Diagnostics & Target Experiments Department  
Sandia National Laboratories  
P.O. Box 5800  
Albuquerque, NM 87185-1196

Abstract

Ion-beam driven hohlraum targets were designed to absorb the energy of PBFAll lithium ion beams within a foam, which converted the ion beam energy into x-rays. The foam was held within a gold hohlraum. X-ray radiation was observed from the top of the target through a circular diagnostic aperture. On the bottom of the target was a gold-coated aluminum witness plate, which was a component of an active, shock-breakout diagnostic. Surrounding the outside of the hohlraum were five titanium pins which produced ion-induced inner-shell x-rays (4.5 keV) to diagnose the lithium beam. Several different manufacturing processes and characterization techniques were utilized to prepare these targets. Extensive documentation provided quality control on their preparation. This report summarizes the preparation, characterization, and documentation of targets for ion-beam driven hohlraum experiments.

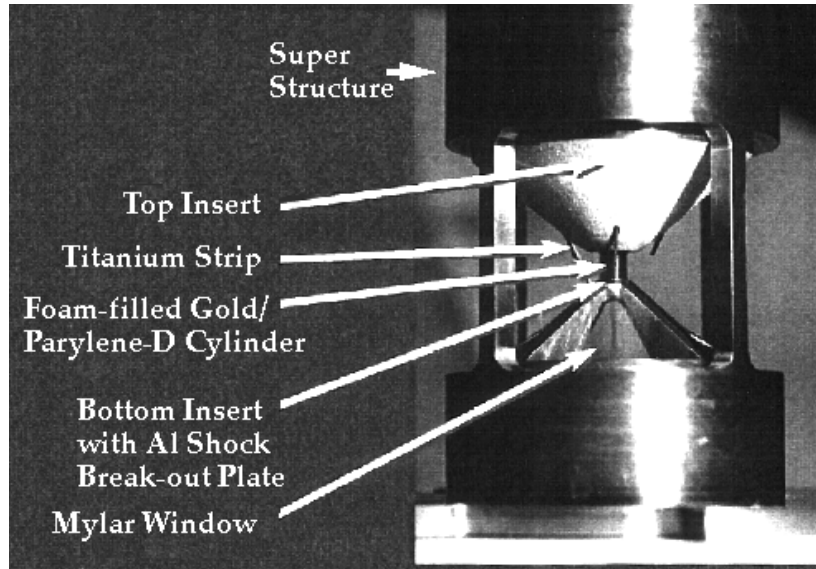
Intentionally Left Blank

## Outline

|    |                                  |
|----|----------------------------------|
| 4  | Introduction                     |
| 5  | Component Preparation            |
| 6  | Hohlraum and Foam Retainer       |
| 8  | Foam                             |
| 8  | Titanium Strips                  |
| 9  | Shock-Breakout Plate             |
| 9  | Assembly Procedure               |
| 11 | Characterization                 |
| 11 | Foam                             |
| 13 | Hohlraum Wall Thickness          |
| 13 | Target Centering and Positioning |
| 16 | Radiography                      |
| 17 | Documentation                    |
| 17 | Conclusions                      |
| 20 | Acknowledgements                 |
| 20 | References                       |
| 22 | Distribution                     |

## Introduction

The thermal x-ray target was designed as a hollow 4 mm diameter right circular cylinder with 1.5 micrometer ( $\mu\text{m}$ ) thick gold walls. The gold cylinder was supported by a thin polymer coating, Parylene-D, and contained a low-density foam with a nominal composition of  $\text{CH}_2$ . The target is shown in Figure 1.



These targets were designed to absorb the energy of the ion beam within the foam, which

converted the ion beam energy into x-rays<sup>1</sup>. X-ray radiation was observed from the top of the target through a circular diagnostic aperture with a diameter of either 1.5 or 3 mm. On the bottom of the target was a gold-coated aluminum witness plate, which was a component of an active, shock-breakout diagnostic. Surrounding the outside of the hohlraum were five titanium pins which produced ion-induced inner-shell x-rays (4.5 keV) to diagnose the lithium beam. At the top of the target, a large, conical, aluminum-coated, brass section (top insert) mechanically supported the hohlraum and intercepted any stray ion beam. At the bottom, another brass conical section (bottom insert), containing 3  $\mu\text{m}$  Mylar, poly(ethylene terephthalate), windows, mechanically supported the hohlraum and provided a vacuum seal. The windows allowed x-ray emission from the titanium pins to be viewed from below. The target was supported in a superstructure machined from brass which mated with the cathode hardware of the PBFA II

Fig. 1. Photograph of the target showing the major components and the supporting super structure.

ion diode. The interior of the hohlraum and diagnostic pathways on the top and bottom were evacuated during the experiment and were designed to withstand a pressure differential of 2 torr.

Several different manufacturing processes were utilized in the preparation of these targets. Many of the components were mechanically weak because of density limitations (areal or volumetric). For example, the hohlraum walls were 4.5  $\mu\text{m}$  thick; yet they had to be wrinkle free over the entire surface and be able to support a small differential pressure. The foam had a density of 5  $\text{mg}/\text{cm}^3$ . For comparison, the density of dry air at 1 atmosphere of pressure is 1.19  $\text{mg}/\text{cm}^3$ . Neither of these components could be handled unless supported by another sacrificial structure. For the hohlraums, our handling philosophy was to prepare it on an extractable mandrel. After evaporating gold onto the mandrel, it was attached to a robust part of the target support structure and only then was the mandrel removed by extraction (dissolution). In the case of the foams, they were prepared with a solvent based process which used a solvent that was solid at room temperature. The solvent-filled foams were easily handled and machined. Only after placement within the hohlraum was the solvent removed by sublimation (freeze-drying). Thereby, the most delicate parts of the target endured no handling, but were supported until after their assembly into the target. Although these techniques made the assembly possible, they complicated characterization. More robust parts of the target were machined with traditional methods including electrical discharge machining. Films and coatings were prepared by chemical or physical vapor deposition and plasma spray.

### Component Preparation

The major physics components of the target included the polymer-coated gold cylinder (hohlraum), the foam retainer (lid to the hohlraum) including its' diagnostic aperture, the

foam, the titanium beam diagnostic pins outside of the hohlraum (“titanium birdcage”), and the aluminum shock-breakout plate. These are shown in figure 2. Details on the other components of the targets can be found in reference 2.

#### Hohlraum and Foam Retainer

The Hohlraum consisted of a hollow polymer-coated gold 4mm diameter right circular cylinder. The foam retainer’s purpose was twofold: to provide precise diagnostic apertures, and to form the lid for the hohlraum which held the foam in place. Both of

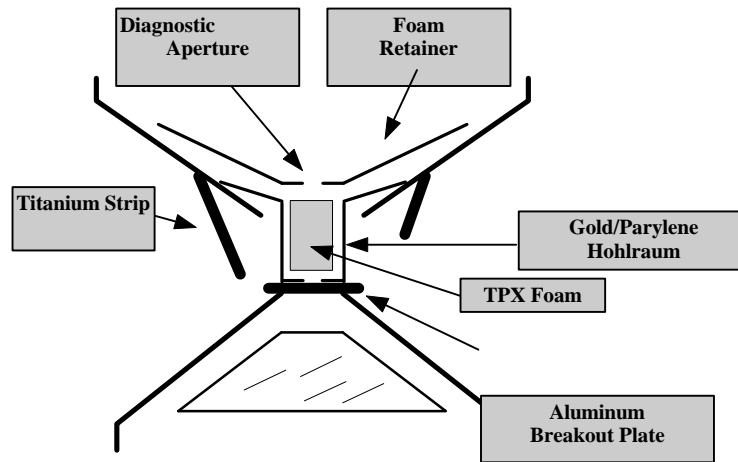


Fig. 2. Illustration of the target’s major components.

these components were prepared in similar ways. First a mandrel of extrusion grade acrylic, poly(methylmethacrylate), was machined and polished to the required shapes. Mandrels were then coated with 1.5  $\mu\text{m}$  (hohlraum) or 2  $\mu\text{m}$  (foam retainer) of 99.999% purity gold in a physical vapor deposition coating chamber using an electron beam source. The mandrels were held in a .5 Hz. rotating fixture and the angle of the mandrels with respect to the source was varied from 90° to 45° to assure uniform



coating on all surfaces . A witness slide was attached to each mandrel stem for subsequent profilometer measurement, and a surplus part of the mandrel coating was also used for direct measurement of the coating thickness. Coated mandrels were checked for pinholes by directing a fiber optic light into the acrylic and observing light emission through the gold coating. Only mandrels which had no pinholes were processed further.

The foam retainer had an extra 12  $\mu\text{m}$  of gold electroplated to bring its thickness up to 14  $\mu\text{m}$ . Gold-coated hohlraum mandrels were coated with 3  $\mu\text{m}$  of Parylene-D, poly(dichloro-para-xylylene)<sup>3</sup>,  $\{-\text{C}_8\text{H}_6\text{Cl}_2-\}_n$ . These mandrels were mounted horizontally onto a rotating fixture inside the Parylene coater. Witness slides were mounted with the mandrels and profilometer measurements were later used to obtain the thickness of coated Parylene-D.

Mandrels for the hohlraum and foam retainer were designed with a stem, to hold and rotate the part, and with sharp edges wherever a cut in the coating was required. These edges were trimmed with a sharp razor at the location of the apertures and the edge of the part. The hohlraum mandrel is shown below with these extra features indicated. The foam retainer mandrel looked similar. Foam retainer mandrels were extracted with acetone and stored until assembly. Hohlraum mandrels were not extracted until after assembly into the top insert because of their delicate structure.

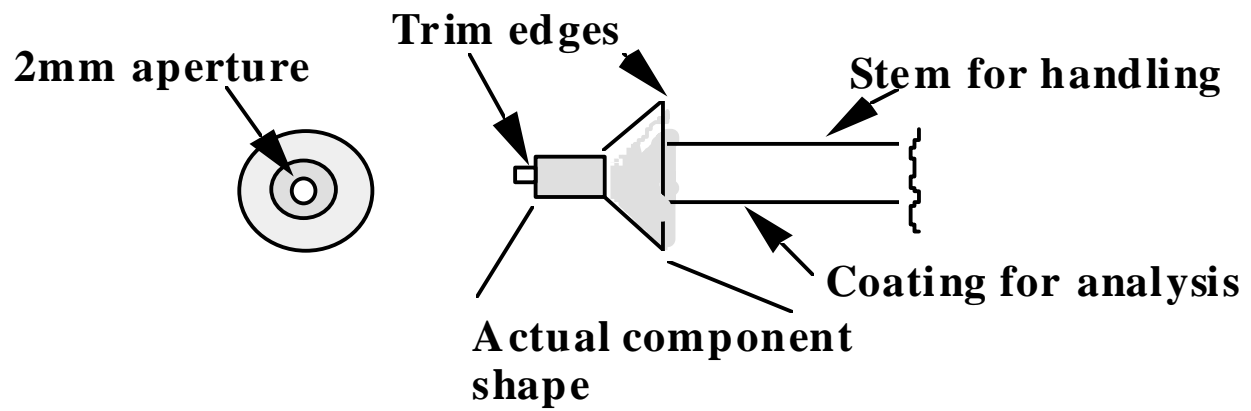


Fig. 3. Hohraum mandrel design.

## Foam

Poly(4-methyl-1-pentene), TPX, foams were obtained from Oak Ridge National Laboratories<sup>4</sup> (ORNL). The foams had a nominal composition of  $\text{CH}_2$  and density of  $5 \text{ mg/cm}^3$ . The foams were prepared with a solvent-based phase separation process whose general features are described elsewhere<sup>5</sup>. In the particular process employed by ORNL, the solvent used was a solid at room temperature with a low vapor pressure (51% naphthalene and 49% durene). The foams were machined at ORNL to the hohlraum dimension (4 mm right circular cylinder) with the solvent filling the porous regions of the foams (approximately 99.5 volume %). These machined solvent-filled foams were then shipped to us under a vapor pressure of the solvents and upon arrival stored in a freezer. This procedure prevented solvent loss and the probable structural damage that would occur in the resulting weak foams.

## Titanium Pins

Titanium beam characterization pins were produced using a wire-EDM (electrical discharge machining) process. Square pins (0.02 inch on a side) were arranged around the hohlraum by bonding one end of each pin into machined holes in the top insert. The strips were angled at  $65^\circ$  from horizontal toward the bottom of the hohlraum in a skeletal cone shape. They were arranged in either of two configurations; 1) three longer (.445 inch length) and two shorter (.255 inch length) strips or 2) all long pins.

## Shock-Breakout Plate

Aluminum shock-breakout plates were prepared by Texas Instruments Custom Optics Division<sup>6</sup> by diamond point machining of Al-6061 alloy, (0.15% Ti, 0.25% Zn, 0.35% Cr, 1.2% Mg, 0.15% Mn, 0.4% Cu, 0.7% Fe, and 0.8% Si). The aluminum was machined to a 5 mm diameter disk with an initial thickness of 150  $\mu\text{m}$ . One surface of the disk was machined to a flat mirror finish. Then a step of 50  $\mu\text{m}$  covering half of the plate was machined into the other side. The total plate thickness was then 150  $\mu\text{m}$  over half of the plate and 100  $\mu\text{m}$  over the other half. The flat side of the plate was coated with chromium (150-200  $\text{\AA}$  for adhesion) and then with 1.5  $\mu\text{m}$  of gold by e-beam evaporative coating. After assembly, the gold coated side formed a part of the bottom of the hohlraum.

## Assembly Procedure

Targets were built from two subassemblies: the bottom insert and the top insert, which were positioned and aligned within the supporting superstructure, i.e., the target body. The bottom insert was composed of a brass structure covered (on the side toward the beam) with 25.4  $\mu\text{m}$  of plasma-sprayed aluminum, with windows in four quadrants. Each window was covered with 3  $\mu\text{m}$  of Mylar. An aluminum shock-breakout plate was attached to the top. Both the shock-breakout plate and the Mylar-covered windows formed vacuum seals.

Once completed, the bottom insert was bonded to the target body. After curing the adhesive, the target body containing this subassembly was placed into a leak check fixture, pressurized to 3 torr with argon, and monitored for 30 minutes. Only

assemblies with a leak rate of less than 0.02 torr/min were accepted and processed further.

The top insert was composed of a brass conical shaped piece coated on its outer surface (facing the incoming beam) with 25.4  $\mu\text{m}$  of aluminum by a plasma spray process. Five pilot holes were placed in the top insert; these were used to locate and secure the titanium strips. A single strip was placed in quadrants one, two, and four, and two strips were placed in quadrant three. The appropriate strips (short or long) were oriented in the top insert by an assembly fixture and bonded in place with a fluorescent-tagged epoxy, (N-methyl pyrrolidione added to fluoresce between 360-400 nm). After curing, the assembly was examined under ultraviolet (UV) light to detect fluorescence from vagrant epoxy. If vagrant epoxy was observed, the adhesive was removed before curing. Once the strips were secured, a hohlraum mandrel was bonded into the top insert with a solvent-resistant epoxy, and then the entire top insert was placed into an acetone bath for extraction of the hohlraum mandrel. A completed top-insert is shown in Figure 4.

Next, the top insert was attached to the target body with the use of another bonding fixture and telescope coupled to a video monitor. The top-insert was mounted on a shaft with the titanium strips positioned in the proper quadrants. The top-insert was then lowered by micrometer adjustment into the target body to enable the bottom of the hohlraum to be secured to the shock breakout plate. The epoxy used also contained a UV tracer. The three bond lines at the hohlraum/shock-breakout plate, the hohlraum/top-insert interface, and the top-insert/target body interface formed vacuum seals. These were checked by leak testing the entire target at this

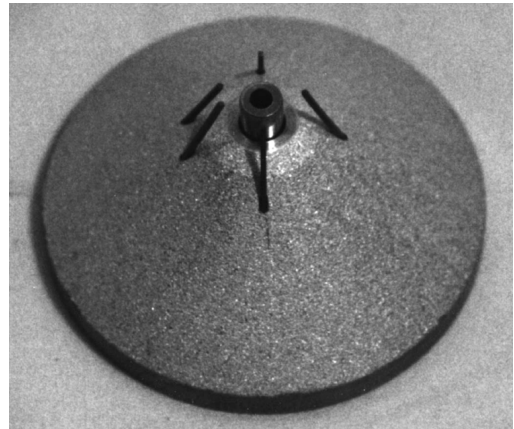


Fig. 4. Completed top insert consisting of an aluminum-coated brass conical support structure, titanium strips, and a parylene-D/gold hohlraum.

time to the same criteria as the bottom insert, i.e., a maximum leak rate of 0.02 torr/min at 3 torr of argon for 30 minutes.

Finally, a solvent-filled foam cylinder was installed into the hohlraum, and then freeze-dried at 15 °C and a vacuum of 25 torr for 30 hours. A foam retainer was bonded into the top-insert to hold the foam in the hohlraum and to provide the diagnostic aperture. A brass debris block completed the target build<sup>2</sup>.

### Characterization

A variety of analytical techniques were used to characterize the hohlraum, foam retainer, titanium strips, and the foam. These included optical measurements, microphotography, scanning electron microscopy, radiography, profilometry, and Rutherford backscattering. Many of the characterizations were destructive and could be performed only on statistically representative samples. The specifications for delivered targets were then inferred from the measurements destructively performed on similar samples. Photographs were taken of all the components, assemblies, and completed targets and were used to document positioning, concentricity, and foil quality.

### Foam

Foam density was calculated from volume and weight measurements of foam bricks. (The cylindrical solvent-filled foam pieces were machined from these same solvent-filled bricks prior to solvent removal.) Volume was determined from optical comparator measurements of the bricks after solvent removal. The bricks were then weighed.

Although the volume of these bricks was two orders of magnitude greater than an individual hohlraum foam, we estimate that the accuracy of this technique to obtain density is approximately five percent due to a lack of parallelism and a rough surface finish. The densities of two bricks were found to be  $4.1 \text{ mg/cm}^3$  and  $4.9 \text{ mg/cm}^3$  (average of  $4.5 \text{ mg/cm}^3$ ; requested density  $5 \text{ mg/cm}^3$ ). This variation may be partly due to variability in the shrinkage of the foams during solvent removal. Typical shrinkage was found to average about 7%. Scanning electron microscopy was performed on a foam sample which was freeze-fractured to preserve its morphology. The foam surfaces were sputtered with a thin gold/palladium layer to reduce charging in the 3 kV electron beam. Cell sizes between five and one hundred  $\mu\text{m}$  were observed as shown the SEM images of Fig. 5.

Photographs were taken of the top of the foam after insertion into the hohlraum and removal of the solvent in order to verify the absence of dirt or visible contaminants and to insure that the shrinkage of the foam was uniform and not excessive. No other characterization could be performed on the actual foams used in the experiments because of their delicate nature. The possibility of using ion microtomography to characterize the density variation within a cylindrical foam sample was investigated. However, this process proved destructive to these particular foams because of the mounting, handling, and transportation required. Solvent-filled foam cylinders were first mounted on a suitable substrate for analysis, the solvent removed, and then transported to the ion tomography equipment. Data was successfully taken for

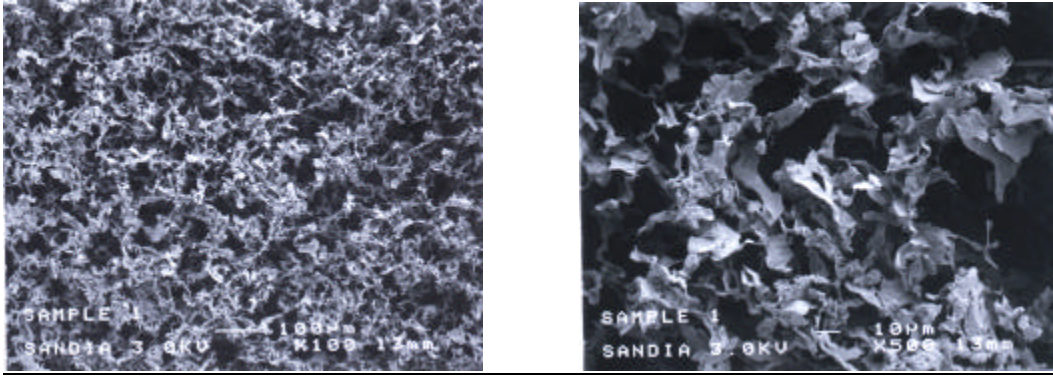


Fig. 5. Scanning electron photomicrographs of nominal  $5\text{mg}/\text{cm}^3$  TPX foam.

purposes of demonstrating the capability of ion tomography on foams of this density. The data showed that density variations as small as 1% could be determined with a spatial resolution of  $10\ \mu\text{m}$ .

#### Hohlraum Wall Thickness

Hohlraum walls were composed of vapor deposited gold and Parylene-D. Thicknesses were determined using a Dektak<sup>®</sup> profilometer on witness slides located very close to the actual parts in the coating chamber. The measurements were made separately; one for the gold coating and one for the Parylene-D. The accuracy of this data is considered to be within ten percent. Rutherford Backscattering Spectroscopy (RBS) was performed on the coating deposited on an excess part of the mandrels, (as seen in Fig. 3). Accuracy for the RBS technique is approximately five percent. Table I contains both profilometry and RBS measurements for each hohlraum. Both the gold and Parylene-D coatings were very close to the design values. The average Parylene-D coating was within 2.7% of the design value and the greatest deviation from the design value was under 11%. The gold thicknesses, as judged by RBS, were also very close to the design value. The greatest deviation was under 15%, while the average gold



thickness was within 5% of the design value. The gold thickness deposited on 75% of the targets was within 5% of the design value and 87.5% were within 10%.

### Target Centering and Positioning

Optical comparator measurements (Gage Master, Series 20) were made on targets to determine the hohlraum height and diameter, the aperture diameter, the vertical and horizontal centering of the hohlraum with respect to the target body, the centering of the aperture with respect to the target body, the angles of the titanium strips, and their length and width. The optical comparator works by projecting a shadow image of the target onto a screen. Dimensions are then determined by a computer controlled positioning program which allows measurement of distances and angles to an accuracy of 2  $\mu\text{m}$ . Some of these measurements are summarized in Table II.

Table I. Hohlraum thickness data for Parylene-D and gold. Design thicknesses were 3  $\mu\text{m}$  Parylene-D and 1.5  $\mu\text{m}$  gold. Deviations (%) from design thicknesses are also shown.

| Target Number            | Dektak <sup>®</sup> Thickness $\mu\text{m}$<br>Gold | Dektak <sup>®</sup> Thickness $\mu\text{m}$<br>Parylene-D | RBS Thickness $\mu\text{m}$<br>Gold |
|--------------------------|---|---|-------------------------------------|
| LT794-4ITF<br>(ITF TEST) | 1.52<br>(+1.3%)                                     | 2.83<br>(-5.7%)   | 1.55<br>(+3.3%)                     |
| LT794-5                  | 1.52<br>(+1.3%)                                     | 2.83<br>(-5.7%)   | 1.55<br>(+3.3%)                     |
| LT794-6                  | 1.54<br>(+2.7%)                                     | 3.32<br>(+10.7%)  | -----                               |
| LT794-8                  | 1.49<br>(-0.7%)                                     | 3.13<br>(+4.3%)   | -----                               |
| LT794-9                  | 1.60<br>(+6.6%)                                     | 3.14<br>(+4.7%)   | 1.29<br>(-14%)                      |
| LT794-10                 | 1.52<br>(+1.3%)                                     | 3.13<br>(+4.3%)   | 1.41<br>(-6%)                       |
| LT794-11                 | 1.51<br>(+0.7%)                                     | 3.13<br>(+4.3%)   | 1.49<br>(-.7%)                      |
| LT794-12                 | 1.53<br>(+2.0%)                                     | 3.13<br>(+4.3%)   | 1.47<br>(-2%)                       |
| LT794-13                 | 1.48<br>(-1.3%)                                     | 2.98<br>(-.7%)  | 1.51<br>(+.7%)                      |
| LT794-14                 | 1.51<br>(+0.7%)                                     | 2.98<br>(-.7%)  | 1.44<br>(-4%)                       |
| LT794-16<br>(RADIOGRAPH) | 1.52<br>(+1.3%)                                     | 3.23<br>(+7.7%)   | -----                               |

|           |                 |                 |                 |
|-----------|-----------------|-----------------|-----------------|
| Y TARGET) |                 |                 |                 |
| Mean      | 1.52<br>(+1.3%) | 3.08<br>(+2.7%) | 1.46<br>(-2.7%) |

Hohlraum diameters closely approximated the designed diameter of 4 mm. Hohlraum height showed more variability because both the top and bottom were bonded with

Table II. Target Component Concentricity.

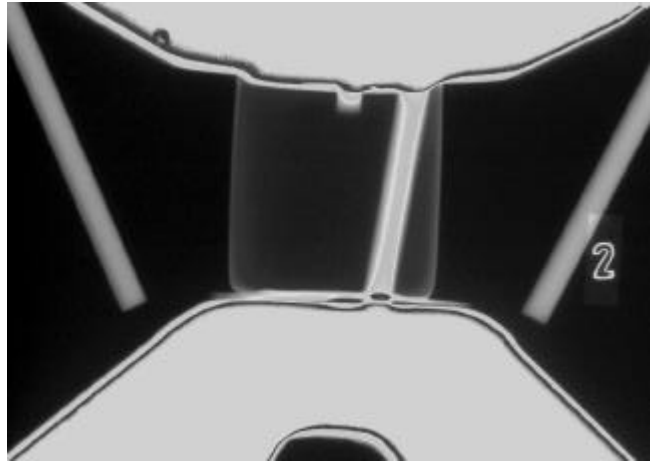
| Target Number | Hohlraum Diameter | Hohlraum off-Center Horizontal | Hohlraum off-Center Vertical | Foam Retainer Aperture                  | Aperture off-Center |
|---------------|-------------------|--------------------------------|------------------------------|---|---------------------|
| Design Value  | 4 mm              | 0.0 mm                         | 0.0 mm                       | 3.0mm or 1.5 mm                         | 0.0 mm              |
| LT794-5       | 4.002             | .1264                          | -.068                        | 3.022                                   | 0.492               |
| LT794-6       | 3.926             | .0365                          | -.039                        | 3.020                                   | 0.292               |
| LT794-8       | 3.968             | .1723                          | -.073                        | 2.998                                   | 0.178               |
| LT794-9       | 4.002             | .0480                          | +.032                        | 3.054                                   | 0.316               |
| LT79410       | 3.996             | .1253                          | .000                         | 3.030                                   | 0.079               |
| LT79411       | 4.004             | .0921                          | -.001                        | 1.610                                   | 0.040               |
| LT79412       | 3.954             | .0510                          | -.061                        | 1.560                                   | 0.242               |
| LT79413       | 3.964             | .0100                          | -.005                        | 1.668                                   | 0.175               |
| LT79414       | 3.958             | .0500                          | +.046                        | 2.984                                   | 0.030               |
| LT79416       | 3.968             | .2233                          | -----                        | 1.498                                   | 0.171               |
| MEAN          | 3.974             | 0.093                          | 0.036                        | 3.018<br>(3 mm) or<br>1.584<br>(1.5 mm) | 0.202               |

epoxy to other components, and the thickness and other factors of the adhesive could change the overall height. The titanium strips were aligned very accurately due to the fixture that was used to secure them. The angle of the strips with respect to horizontal in two viewed directions (viewed by looking toward the center of the hohlraum and at 90° to this view) was always within 3° of the designed angle and in the majority of cases was within 1°.

Hohlraum centering was calculated from optical comparator measurements of distances from the target body to the hohlraum edge at two positions (90° apart). Hence, the off-center number is only an estimate based upon these two data points. In general the hohlraum was centered horizontally almost perfectly. The average deviation was less than 0.1 mm. Vertical centering in the cathode hardware was totally dependent on the size of the spacer used. Based upon optical comparator positioning information, we chose a spacer size which yielded an average deviation in the vertical centering of less than 0.04 mm. This was well within our diagnostic resolution.

Aperture diameters and centering were measured in a similar way. Only two measurements (at 90° apart) were used to estimate the centering of the apertures. The diameters were very close to the desired design values. For the 3 mm diameter aperture the average deviation from this design was only 0.6%. For the 1.5 mm diameter apertures the average deviation from this design was significantly greater but still under 6%. The apertures were off-center by an average of 0.2 mm, with significant variability.

Fig. 6. Technique used to image the distance from the pins to the gold foil: 35 kV, 500  $\mu$ A, 165-second exposure time; source-to-object distance: 2-1/8 " ; source-to-film: 27 ". A hard cassette was used with Kodak AA film sandwiched between .001 " of lead foil with .010 " of lead screen behind the foil to reduce scatter.



## Radiography

Radiography, digitization, and colorization was performed on a single target, #LT794-16, that was fabricated specifically for this purpose. It was considered representative of all delivered targets. One of the radiographs showing the distance from the titanium pins to the gold foil is shown in Figure 6.

## Documentation

Documentation occurred at all stages of the assembly process in order to provide both archival information and quality control measures on the process. The components and the subassemblies had associated documentation; details of preparation and characterization were recorded and this “traveler” remained with its component throughout the assembly process. The target assembly was also documented on an “assembly sheet,” which verified that every step was completed, all characterizations were performed, and all data recorded. Some methods of characterization were documented separately. With each delivered target, a “delivery sheet,” containing some of the most important target specifications, was included. Table III summarizes the sequence of targets shot on PBFA II and their most pertinent configurational information. Finally, a target assembly procedure was written at the end of the build to document, for archival purposes, the details of the assembly process and all of the characterization results<sup>2</sup>. All travelers, characterization results, and delivery sheets are archived in folders for future reference. In addition, numerous parts have been archived, including: the witness slides from all coatings and the radiography target. These parts are available to answer any materials questions which could arise when data is analyzed in the future.

## Conclusions

Due to the delicate nature of the Hohlraum’s foil and foam, and available analytical techniques, these components could not be directly characterized without destroying them. Instead, these components were characterized by gathering data on similar materials, and extrapolating these results to the actual target components. Other

aspects of the targets were characterized nondestructively. A total of nine targets were delivered and shot for this series.

Table III. The sequence of targets shot on PBFA II.

| Shot Sequence | DAS Shot Number | Pre-Shot Number | Target Number | Aperture Diameter (mm) | Pin Configuration | Delivery or Shot Date |
|---------------|-----------------|-----------------|---------------|------------------------|-------------------|-----------------------|
| 1             | 6501            | 2025            | LT794-5       | 3.0                    | all long          | delivered 7-13-94     |
| 2             | 6517            | 2026            | LT794-6       | 3.0                    | 2 short; 3 long   | delivered 7-21-94     |
| 3             | 6529            | 2027            | LT794-8       | 3.0                    | 2 short; 3 long   | delivered 7-27-94     |
| 4             | 6542            | 2028            | LT794-9       | 3.0                    | 2 short; 3 long   | shot 8-9-94           |
| 5             | 6547            | 2029            | LT794-10      | 3.0                    | 2 short; 3 long   | shot 8-11-94          |
| 6             | 6551            | 2030            | LT794-11      | 1.5                    | 2 short; 3 long   | shot 8-12-94          |
| 7             | 6554            | 2031            | LT794-12      | 1.5                    | 2 short; 3 long   | delivered 8-12-94     |
| 8             | 6560            | 2032            | LT794-13      | 1.5                    | 2 short; 3 long   | delivered 8-16-94     |
| 9             | 6569            | 2033            | LT794-14      | 3.0                    | 2 short; 3 long   | delivered 8-18-94     |

We obtained excellent data on the vertical and horizontal positioning of the hohlraums. Deviations from horizontal positioning from the design were, at most, tenths of a millimeter, and deviation from vertical were negligible. From a fabrication standpoint, the targets were perfectly centered. The Parylene-D/gold hohlraums were the correct size and had no visible flaws such as wrinkles or discoloration. Wall thicknesses of the hohlraums were very close to the design specifications in all cases. Maximum deviations of Parylene-D thickness from design thickness was under 10% and for gold was under 15%, but the majority were much closer. Titanium pins were the correct size and had near-perfect alignment due to the bonding fixture which was used.

One weak area in our characterization was in the measurement of the top aperture size and circularity. We measured two diameters of the top aperture at 90° from each other and then averaged these to compare to the desired value. This gave us no information on the uniformity of the diameter (i.e. circularity), although photography allowed us to keep a permanent visual record. If targets of this type were used in the future, it would be important to develop a system to completely evaluate the shape of the aperture, the quality of its edge, and the area that it circumscribes. These apertures were formed by cutting a gold foil with a scalpel. This worked quite well for the 3 mm diameter apertures, but was less accurate for the 1.5 mm diameter apertures. For the future, we need to develop a more accurate method of cutting the foil. Possible candidates are laser or e-beam machining.

The low-density foam may be the most important physics component of this target. But by far the weakest area of this target build was the foam preparation and characterization, including its density, density uniformity, and even volume. We should spend more effort to develop the technology to prepare these low-density foams for future targets. (Another problem that will not be discussed here, but with very serious repercussions, was the occasional contamination of targets by foreign materials during insertion into PBFA II.)



Characterization of the foams was very limited. Better preparation of foam blocks for density analysis is required. These blocks were removed from the main foam brick and were shaped by hand to form a parallelepiped. A more accurate method would be to have several extra target pellets machined, accurately measure and weigh them, and calculate numerous densities that could be averaged. In addition, a statistical evaluation should be made of the foam sampling technique to obtain the best specimens for analysis.

No information on density uniformity was obtained, although ion microtomography may be promising in some future instances. This technique should be developed, optimally as a nondestructive test, to obtain direct information about density and density uniformity. For example, if the foam could be permanently attached to a rigid base, it could be transported to the ion microtomography beam and then returned for use as a characterized target if the base were a part of the target design.

### Acknowledgements

Paul Baca contributed significantly to this project. We sincerely appreciate the efforts of Bonnie McKenzie and Gary Zender for the SEM photos, Art Pontau and Arlyn Antolak for their work demonstrating ion microtomography, Deanna Sevier and Kyle Thompson for radiography, George Arnold for RBS, Bob Henning for plasma spray, and the projects machining department. All of their dedicated efforts were needed for the success of this target series.

### References

1. T. A. Mehlhorn, Ion Beam Coupling and Target Physics Experiments at Sandia National Laboratories,” in “Laser Interaction & Related Plasma Phenomena,” ed by G. H. Miley & H. Hora, 10 (1992).
2. P. S. Sawyer, P. M. Baca, M. Smith, and J. H. Aubert, “1994 Lithium Thermal Target Assembly Procedure,” communication of Sandia National Laboratories, 1994.
3. M. Szwarc, Polym. Eng. and Sci., 16 (7), 473 (1976).
4. Manufactured by Ron Simandl, Oak Ridge National Laboratories, Oak Ridge, Tennessee.
5. J. H. Aubert and A. P. Sylwester, “Microcellular foams? Here’s How!,” CHEMTECH, 21, 290 (1991).
6. Manufactured by George Platt, Texas Instruments Custom Optics Division, Dallas, Texas.

UNLIMITED RELEASE  
INITIAL DISTRIBUTION

Internal Distribution:

|   |         |   |
|---|---------|---|
| 1 | MS-1196 | G. A. Chandler, 9577                            |
| 1 | MS-1196 | A. R. Moats, 9577                               |
| 5 | MS-1196 | M. L. Smith, 9577                               |
| 1 | MS-1187 | R. J. Dukart, 9571                              |
| 1 | MS-1196 | T. E. Alberts, 9577                             |
| 1 | MS-1196 | D. E. Hebron, 9577                              |
| 5 | MS-1407 | J. H. Aubert, 1815                              |
| 5 | MS-1349 | P. S. Sawyer, 1815                              |
| 1 | MS-0734 | P. M. Baca, 6472                                |
| 1 | MS-1435 | H. J. Saxton, 1800                              |
| 2 | MS-0619 | Review and Approval Desk, 12690<br>For DOE/OSTI |
| 5 | MS-0899 | Technical Library, 4916                         |
| 1 | MS-9018 | Central Technical Files, 8940-2                 |